

两例基于相同的含氮及联苯二羧基混合配体构筑的 Zn(II)/Cd(II)配位聚合物:不同的穿插结构和荧光性质

卢久富* 许宇航 靳玲侠 郭小华 赵蔡斌 郑楠 姜敏 葛红光*

(陕西理工大学化学与环境科学学院,陕西省催化基础与应用重点实验室,汉中 723001)

摘要: 在溶剂热条件下合成了 2 个锌(II)/镉(II)配位聚合物: $\{[\text{Zn}(\text{1,3-bip})(\text{bpdc})] \cdot 0.5\text{H}_2\text{bpdc}\}_n$ (**1**), $\{[\text{Cd}_2(\text{1,3-bip})_2(\text{bpdc})_2] \cdot \text{DMF}\}_n$ (**2**), H_2bpdc =4,4'-联苯二甲酸, 1,3-Bip=1,3-二(咪唑基)丙烷。并通过 X 射线单晶衍射,粉末 XRD、红外光谱、元素分析以及热重分析对其结构进行表征。单晶解析结果表明:配位聚合物 **1** 是一个五重穿插 3D→3D 三维空间网络结构,配位聚合物 **2** 是一个二重穿插的 2D→2D 二维的(4,4)网格层状结构。另外,研究了 2 个配位聚合物在室温下的热稳定和荧光性能。

关键词: 溶剂热合成; 配位聚合物; 双咪唑; 拓扑; 荧光性能

中图分类号: O614.24*1; O614.24*2

文献标识码: A

文章编号: 1001-4861(2017)01-0115-08

DOI: 10.11862/CJIC.2017.001

Two Zn(II)/Cd(II) Complexes Constructed by the Same Biphenyl-dicarboxylate and N-Donor Ligands: Different Interpenetrating Structures and Photoluminescence Properties

LU Jiu-Fu* XU Yu-Hang JIN Ling-Xia GUO Xiao-Hua

ZHAO Cai-Bin ZHENG Nan JIANG Min GE Hong-Guang*

(Shaanxi Province Key Laboratory of Catalytic Foundation and Application, College of Chemical &
Environment Science, Shaanxi Sci-Tech University, Hanzhong, Shaanxi 723001, China)

Abstract: Two metal coordination polymers, namely $\{[\text{Zn}(\text{1,3-bip})(\text{bpdc})] \cdot 0.5\text{H}_2\text{bpdc}\}_n$ (**1**), $\{[\text{Cd}_2(\text{1,3-bip})_2(\text{bpdc})_2] \cdot \text{DMF}\}_n$ (**2**), where 1,3-bip=1,3-bis(imidazol)propane, H_2bpdc =biphenyl-4,4'-dicarboxylic acid, were synthesized by changing the central ion with the same mixed ligands under solvothermal conditions. The complexes were further characterized by single crystal X-ray diffraction, powder XRD, FTIR, TGA and elemental analysis techniques. Single crystal X-ray analysis revealed that complex **1** exhibits a 5-fold 3D→3D parallel interpenetrating frameworks. Complex **2** features a 2D→2D (4,4) net, which are interlocked with each other to form a 2-fold parallel interpenetrating 2D architecture. The varieties in coordination numbers of the central metals are the key reasons for the structural differences. In addition, the photoluminescence properties of **1** and **2** in the solid state at room temperature were also investigated. CCDC: 1011050, **1**; 1013480, **2**.

Keywords: solvothermal synthesis; coordination polymers; interpenetrating frameworks; photoluminescence properties

收稿日期: 2016-02-14。收修改稿日期: 2016-09-22。

国家青年自然科学基金(No.21603133)、陕西理工大学博士启动经费(No.SLGKYQD2-13,SLGKYQD14-10)和陕西理工大学校级项目(No.SLGKY15-36)资助。

*通信联系人。E-mail: jiufulu@163.com, gehg@sntu.edu.cn

Construction of new metal coordination polymers (MCPs) has attracted attention due to their diverse structural topologies and potential applications as functional materials such as gas storage, magnetism, catalysis, and luminescence^[1-5]. Metal-directed self-assembly to construct rigid and robust metal-organic polymers (MCPs) has provided an extensive class of solid materials with high stability and desired physical properties^[6-8]. Within this context, interpenetration and polycatenation networks with optimal functionalities have attracted particular attention. Interpenetrating net can be described as a series of independent nets that penetrate mutually and polycatenation nets can be described molecules with loops through loops. The structures of interpenetration and polycatenation arrays not only provide interesting topological structures but also exhibit promising applications as superhard materials for their peculiar magnetic, optical, and catalytic properties, etc^[9-12].

In recent years, the direct use of two types of organic ligands have been found to be an effective method for the synthesis of MCPs, because of their rich coordination modes, including monodentate, bridging and chelating^[13-14]. To date, many MCPs have been prepared on the basis of carboxylate-type O-donors and amine- or N-donors. Thereinto, Diphenic acid as O-donor ligand has received much attention in the designed synthesis of coordination polymers^[15-17], for example, biphenyl-4,4'-dicarboxylic acid ($H_2bpd c$) is a good candidate for construction of coordination polymers. Meanwhile, flexible bis (imidazole) ligands (such as 1,2-bis(imidazole) ethane (1,2-bie), 1,3-bis(imidazole)propane (1,3-bip), 1,4-bis(imidazole)butane (1,4-bib), 1,5-bis(imidazole)pentane (1,5-bip), 1,6-bis(imidazole)hexane (1,6-bih) and 1,4-bis(imidazol-1-ylmethyl) benzene (bix)^[18-21]) bearing alkyl spacers are good choice of N-donor ligands, in which the flexible nature of spacers allows the ligands to bend and rotate when it coordinates to metal centers, and this often causes the structural diversity and different capacities of spatial extension.

In this paper, we report the metal ions induced synthesis of two new complexes, $\{[Zn(1,3-bip)(bpd c)] \cdot$

$0.5H_2bpd c\}_n$ (**1**) and $\{[Cd_2(1,3-bip)_2(bpd c)_2] \cdot DMF\}_n$ (**2**), constructed by using the same biphenyl-4,4'-dicarboxylic acid and 1,3-bis(imidazole)propane as the mixed ligands.

1 Experimental

1.1 Materials and measurements

All reagents used in the syntheses were of analytical grade. Elemental analyses for carbon, hydrogen, and nitrogen atoms were performed on a Vario EL III elemental analyzer. The infrared spectra ($4\ 000 \sim 400\text{ cm}^{-1}$) were recorded by using KBr pellet on an Avatar 360 E.S.P. IR spectrometer. Thermogravimetric analysis (TGA) was performed on a TGA-SDT Q600 thermal analyzer under N_2 atmosphere with a heating rate of $10\text{ }^\circ\text{C} \cdot \text{min}^{-1}$ in the range of $30 \sim 1\ 000\text{ }^\circ\text{C}$. The fluorescence spectra of samples were measured with a Hitachi F-4500 fluorescence spectrophotometer at room temperature using powder crystal samples.

1.2 Synthesis of complex

1.2.1 Synthesis of $\{[Zn(1,3-bip)(bpd c)] \cdot 0.5H_2bpd c\}_n$ (**1**)

A mixture of $Zn(NO_3)_2 \cdot 6H_2O$ (0.2 mmol, 58.2 mg), 1,3-bip (0.20 mmol, 35.2 mg), NaOH (0.2 mmol, 8 mg) and $H_2bpd c$ (0.20 mmol, 58.2 mg) in DMF- H_2O (6 mL, 1:1, V/V) binary solvent was placed in a 25 mL Teflon-lined stainless steel container, which was heated at $150\text{ }^\circ\text{C}$ for 3 d, and then cooled to room temperature over 24 h. Colourless block crystals of **1** were collected. Yield: 75% based on Zinc. Elemental analysis Calcd. for $C_{30}H_{25}ZnN_4O_6(\%)$: C 59.81, H 4.15, N 9.30; Found (%): C 59.36, H 3.96, N 9.81. IR(cm^{-1}): 3 442(w), 3 125(m), 2 919(w), 1 693(s), 1 612(s), 1 532(m), 1 382(s), 1 252(s), 1 105(m), 852(m) and 763(m).

1.2.2 Synthesis of $\{[Cd_2(1,3-bip)_2(bpd c)_2] \cdot DMF\}_n$ (**2**)

The preparation of **2** was similar to that of **1** except that $Zn(NO_3)_2 \cdot 6H_2O$ was replaced by $Cd(NO_3)_2 \cdot 4H_2O$ (0.20 mmol, 61.6 mg). Colourless block crystals of **2** were obtained. Yield: 75% based on Cadmium. Elemental analysis Calcd. for $C_{49}H_{47}Cd_2N_9O_9(\%)$: C 52.00, H 4.16, N 11.14; Found(%): C 52.36, H 4.02, N 11.41. IR(cm^{-1}): 3 444(w), 3 111(m), 2 919(w), 2 865(w), 1 671(m), 1 585(m), 1 524(s), 1 393(s), 1 238(w),

1 088(m), 846(m) and 771(m).

1.3 Determination of crystal structures

Crystals of **1** (0.22 mm×0.18 mm×0.14 mm) and **2** (0.23 mm×0.18 mm×0.14 mm) were carefully selected under an optical microscope, and data collection were performed on a CCD automatic diffractometer with graphite-monochromatized Mo $K\alpha$ radiation ($\lambda = 0.071\ 073\ \text{nm}$) by using the ω -scan mode at room

temperature. An empirical absorption correction was applied using the Semi-empirical from equivalents program^[22]. The structures were both solved by direct methods using SHELXS-97^[23]. Crystallographic data for **1** and **2** are presented in Table 1. The main bond lengths and angles are listed in Table 2.

CCDC: 1011050, **1**; 1013480, **2**.

Table 1 Crystallographic data and structure refinement for **1** and **2**

Compounds	1	2
Formula	C ₃₀ H ₂₅ ZnN ₄ O ₆	C ₄₉ H ₄₇ Cd ₂ N ₉ O ₉
Formula weight	602.90	1 130.78
T / K	293(2)	293(2)
Crystal system	Monoclinic	Monoclinic
Space group	$C2/c$	$P2_1/c$
a / nm	2.261 31(5)	1.537 18(5)
b / nm	1.724 26(5)	2.873 15(9)
c / nm	1.361 89(3)	1.103 94(4)
$\beta / (^\circ)$	94.122(2)	93.025(4)
V / nm^3	5.296 4(2)	4.868 8(3)
Z	4	4
$D_c / (\text{g} \cdot \text{cm}^{-3})$	1.510	1.543
$F(000)$	2 480	2 288
GOF on F^2	1.093	1.105
Reflection, unique	4 654, 370	8 551, 624
$R_1, wR_2^* [I > 2\sigma(I)]$	0.048 5, 0.108 3	0.069 1, 0.150 0
R_1, wR_2^* (all data)	0.070 9, 0.118 2	0.084 9, 0.156 0

$$^*R_1 = \sum (|F_o| - |F_c|) / \sum |F_o|, wR_2 = [\sum (|F_o|^2 - |F_c|^2)^2 / \sum w(F_o^2)]^{1/2}$$

Table 2 Selected bond lengths (nm) and angles ($^\circ$) for **1** and **2**

1					
Zn(1)-O(1)	0.196 0(2)	Zn(1)-N(4)	0.199 1(3)	Zn(1)-N(1)	0.202 2(3)
Zn(1)-O(3)	0.196 7(2)				
O(1)-Zn(1)-O(3)	110.05(10)	O(3)-Zn(1)-N(4)	103.25(7)	O(3)-Zn(1)-N(1)	106.22(11)
O(1)-Zn(1)-N(4)	117.16(11)	O(1)-Zn(1)-N(1)	98.32(12)	N(4)-Zn(1)-N(1)	109.92(12)
2					
Cd(1)-O(1)	0.235 4(5)	Cd(1)-N(1)	0.224 5(9)	Cd(2)-O(7)	0.228 2(6)
Cd(1)-O(2)	0.232 8(5)	Cd(1)-N(4)	0.227 5(8)	Cd(2)-O(8)	0.239 3(6)
Cd(1)-O(3)	0.252 4(6)	Cd(2)-O(5)	0.236 8(5)	Cd(2)-N(5)	0.228 3(6)
Cd(1)-O(4)	0.224 3(5)	Cd(2)-O(6)	0.238 2(5)	Cd(2)-N(8)	0.228 4(6)
O(4)-Cd(1)-N(1)	102.0(3)	O(4)-Cd(1)-O(2)	156.7(3)	N(5)-Cd(2)-N(8)	96.3(2)
O(4)-Cd(1)-N(4)	103.2(3)	O(7)-Cd(2)-N(5)	98.5(2)	O(7)-Cd(2)-O(5)	147.8(2)
N(1)-Cd(1)-N(4)	98.6(3)	O(7)-Cd(2)-N(8)	114.3(2)		

Symmetry codes: ⁱ $-x, y, -z+1/2$; ⁱⁱ $x+1/2, y+1/2, z$; ⁱⁱⁱ $-x+1/2$ for **1**; ⁱ $-x, y+1/2, -z+1/2$; ⁱⁱ $-x, -y, -z$; ⁱⁱⁱ $x, -y-1/2, z-1/2$ for **2**

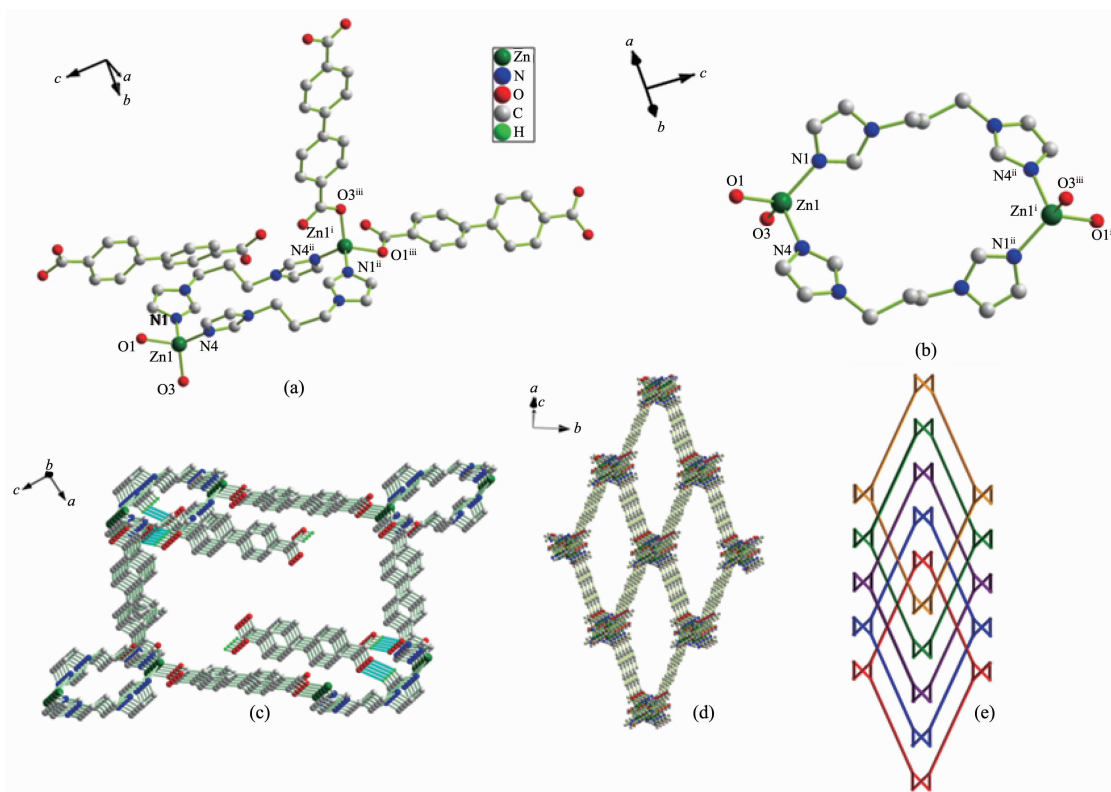
2 Results and discussion

2.1 Description of the structures

2.1.1 Crystal structural description of **1**

Single X-ray diffraction study revealed that complex **1** was isostructural with $\{[\text{Co}(\text{1,3-bip})(\text{bpdc})] \cdot 0.5\text{H}_2\text{bpdc}\}_n$, which has been previously reported by our group^[17]. The asymmetric unit of **1** is composed of a four-coordinate Zn(II) center, a 1,3-bip ligand, a bpdc^{2-} ligand and a half uncoordinated H_2bpdc molecule (Fig.1a). Zn1 ion adopts a distorted tetrahedral geometry, coordinating to two nitrogen donors of two 1,3-bip ligands and two oxygen donors of two bpdc^{2-} ligands (Zn1-O1 0.196 0(3) nm, Zn1-O3 0.196 7(4) nm, Z1-N1 0.202 2 nm, Z1-N4 0.199 1 nm). Both Zn-N and Zn-O bond lengths are well-matched to those observed in similar complexes^[24-26]. Then, 1,3-bip ligand adopts a bis-monodentate bridging mode connecting two Zn(II) centers to form a $[\text{Zn}(\text{1,3-bip})]_2^{4+}$ macrocyclic unit (Fig.1b). Neighboring $[\text{Zn}(\text{1,3-bip})]_2^{4+}$ macrocyclic

unit as a 4-connected secondary building unit are further linked by two conformations of bpdc^{2-} ligands in which the two phenyl rings about the central bond have a twist with a dihedral angle of 0° and 41.02° to form a 12-connected oblong building unit $\{[\text{Zn}_2(\text{1,3-bip})_2]_6(\text{bpdc})_6\}$, and the uncoordinated H_2bpdc molecules are bound inside the pores with intermolecular $\text{O}-\text{H} \cdots \text{O}$ hydrogen bonding interactions ($\text{O}_{\text{H}_2\text{bpdc}}-\text{H} \cdots \text{O}_{\text{bpdc}}$) between O atom of the coordinated bpdc^{2-} ligand and O atom of uncoordinated H_2bpdc molecule with $\text{O} \cdots \text{O}$ distances of 0.262 6 nm (Fig.1c). The bpdc^{2-} acts as a bridging ligand with bis-monodentate coordination mode connecting above-mentioned 12-connected oblong building unit to form the porous 3D architecture (Fig. 1d). From the topological perspective, the $[\text{Zn}(\text{1,3-bip})]_2^{4+}$ macrocyclic unit can be considered as a 4-connected uninodal node with a Schläfli symbol of $(6^5, 8)$ cds type topology. By mutual interpenetration of five independent equivalent frameworks, it leads to



Some hydrogen atoms are omitted for clarity; Symmetry codes: ⁱ $-x, y, -z+1/2$; ⁱⁱ $x+1/2, y+1/2, z$; ⁱⁱⁱ $-x+1/2, y+1/2, -z+1/2$ in (a)

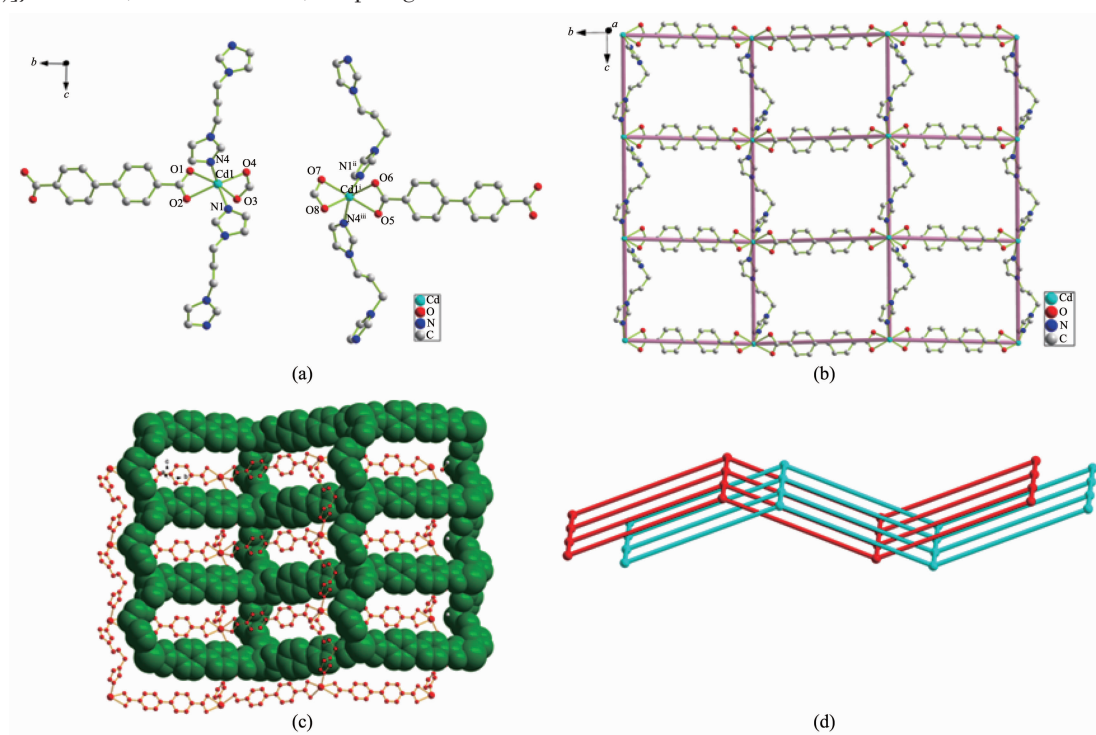
Fig.1 (a) Coordination environment of Zn(II) ion in **1**; (b) View of a 4-connected second building unit of $[\text{Zn}(\text{1,3-bip})]_2^{4+}$; (c) View of uncoordinated H_2bpdc molecules encapsulated in the pore of the 3D framework of **1**; (d) View of the 3D network along the c axis in **1**; (e) 5-fold 3D→3D parallel interpenetrating structure of **1**

the formation of 5-fold 3D \rightarrow 3D parallel interpenetrating architecture (Fig.1e).

2.1.2 Crystal structural description of **2**

The complex **2** crystallizes in the monoclinic system with $P2_1/c$ space group. Each asymmetric unit of **2** contains two Cd(II) ion, two bpdc²⁻ anions, two 1,3-bip ligands and one DMF molecule. As shown in Fig.2a, the two Cd(II) ion exhibit same coordination geometry and are coordinated by four carboxylate O atoms (Cd-O 0.228 2(6)~0.252 4(6) nm) from two bpdc²⁻ anions as the chelate form and two N atoms (Cd-N 0.224 5(9)~0.228 4(6) nm) from two 1,3-bip ligands, showing a distorted octahedral geometry. Each 1,3-bip acts as a bridging ligand coordinating the adjacent Cd(II) ion to form a one dimensional $\{[\text{Cd}(1,3\text{-bip})]\}_n^{2n+}$ chain, where the 1,3-bip ligands show

the *cis*-conformation with the same Cd \cdots Cd distance of 1.109 4(9) nm. These chains are further linked by bridging bpdc²⁻ ligands to generate a 2D infinite undulated rectangular (4,4) grid incorporating a $[\text{Cd}_4(1,3\text{-bip})_2(\text{bpdc})_2]$ window of 1.109 nm \times 1.524 nm based on the Cd \cdots Cd distances (Fig.2b). Then a pair of identical 2D single nets are interlocked with each other to form a 2-fold parallel interpenetrated 2D architecture by (C_{bip}-H \cdots O_{bpdc} 0.234 8, 0.247 0, 0.255 5, 0.258 2, 0.271 9 nm) hydrogen bonds (Fig.2c and d), in which the DMF molecules are resided. Although the two MCPs were constructed by the same carboxylate and N-donor ligand, coordination modes are quite different, resulting in variable framework of the structures, respectively.



Hydrogen atoms are omitted for clarity; Symmetry codes: ⁱ $-x, y+1/2, -z+1/2$; ⁱⁱ $-x, -y, -z$; ⁱⁱⁱ $x, -y-1/2, z-1/2$

Fig.2 (a) Coordination environment of Cd(II) ion in **2**; (b) View of 2D infinite undulated rectangular (4,4) grid in **2**; (c) Perspective view of the 2D coordination network along the *a* axis in **2**; (d) Schematic view of the 2-fold interpenetrating along the *b* axis in **2**

2.2 FTIR spectra, X-ray powder diffraction patterns and thermal properties

As shown in Fig.3, the middle band at 3 442 cm⁻¹ for **1** further indicates the presence of hydron band between uncoordinated dicarboxylate ligand and

molecular skeleton. The weak bands at 3 444 cm⁻¹ for **2** can be assigned to N-H stretching frequency of DMF molecule. The middle band at 3 111 cm⁻¹ and strong band at 1 693 cm⁻¹ belong to O-H and C=O stretching vibration band of uncoordinated

dicarboxylate ligand, respectively. The strong peak at $1\,382\text{ cm}^{-1}$ for **1** and $1\,393\text{ cm}^{-1}$ for **2** indicate the presence of deprotonated -COO^- groups. The peaks at $1\,585$ and $1\,393\text{ cm}^{-1}$ for **2** correspond to the asymmetric and symmetric vibration of the carboxylate group (COO^-), and the difference of the value between them is less than 200 cm^{-1} , which indicates that the carboxylate groups behave as the chelate coordination modes^[27].

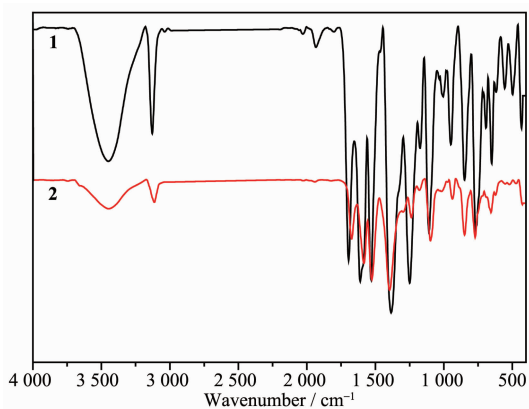


Fig.3 FTIR spectra of complexes **1** and **2**

Fig.4 and 5 show the powder XRD patterns of as-synthesized compounds and the simulated patterns on the basis of single-crystal structures of **1** and **2**, respectively. The diffraction peaks on patterns correspond well in position, indicating the phase purity of the as-synthesized samples.

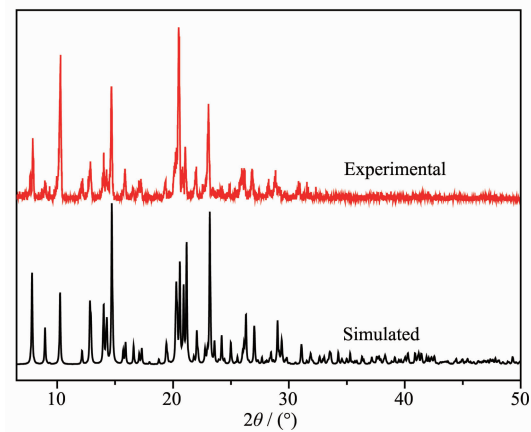


Fig.4 XRD pattern of complex **1**

Thermogravimetric (TG) measurements were carried out from 30 to $1\,000\text{ }^{\circ}\text{C}$ under N_2 atmosphere flow with a heating rate of $10\text{ }^{\circ}\text{C}\cdot\text{min}^{-1}$. As shown in Fig.6, the framework of complex **1** is stable up to $350\text{ }^{\circ}\text{C}$

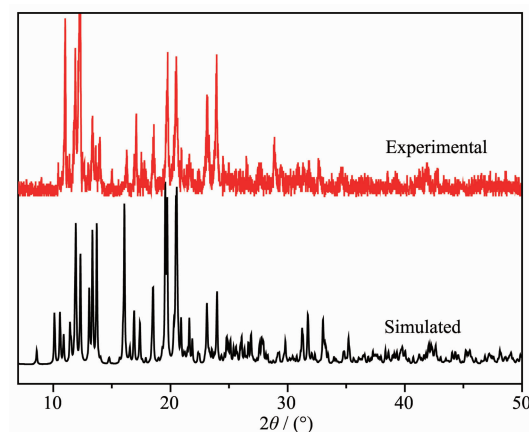


Fig.5 XRD pattern of complex **2**

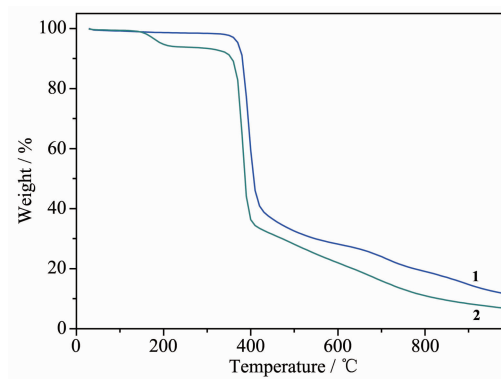


Fig.6 TG curves of complexes **1** and **2**

$^{\circ}\text{C}$ and then the framework begins to collapse. A subsequent weight loss of 88.2% in the temperature range of $350\sim 980\text{ }^{\circ}\text{C}$ corresponds to the release of coordinated 1,3-bip, bpdc^{2-} ligands and a half uncoordinated H_2bpdc molecule (Calcd. 89.3%). Complex **2** exhibits a weight loss of 6.07% from 100 to $230\text{ }^{\circ}\text{C}$, corresponding to the loss of one free DMF molecule (Calcd. 6.45%). It is stable up to about $350\text{ }^{\circ}\text{C}$ and then the framework starts to collapse after that temperature. The ultimate frameworks of **1** and **2** can be stabilized up to $350\text{ }^{\circ}\text{C}$, which are larger than the usual non-interpenetration and polycatenation structures^[28].

2.3 Fluorescence properties

The solid-state luminescence properties of complexes **1** and **2** as well as the free 1,3-bip ligand were investigated at room temperature. Free 1,3-bip shows emission with a maximum at 462 nm upon excitation at 330 nm in solid state, matching with the previous reports^[19]. As shown in Fig.7, the maximum emission peaks for complexes **1** and **2** are observed at

458 and 460 nm upon excitation at 330 nm, respectively, which show slight blue shift in wavelength compared with 1,3-bip ligand. The blue shift of the emission maximum between the complex and the ligand may originate from the coordination of the ligand to the metal centers. The Zn(II)/Cd(II) ion are difficult to oxidize or reduce because of the d^{10} configuration. So the emissions of these MCPs are neither metal-to-ligand charge transfer (MLCT) nor ligand-to-metal charge transfer (LMCT) in nature^[29-30]. Thus, they may be assigned to a mixture characteristics of intraligand and ligand-to-ligand charge transition (LLCT), as reported for other Zn(II) MCPs constructed from mixed N-donor and O-donor ligands^[31]. The enhancement of luminescence in d^{10} complexes may be attributed to ligand chelation to the metal center which effectively increases the rigidity of the ligand and reduces the loss of energy by radiationless decay. The difference of the emission behaviors for **1** and **2** probably derives from the differences in the rigidity of solid-state crystal packing.

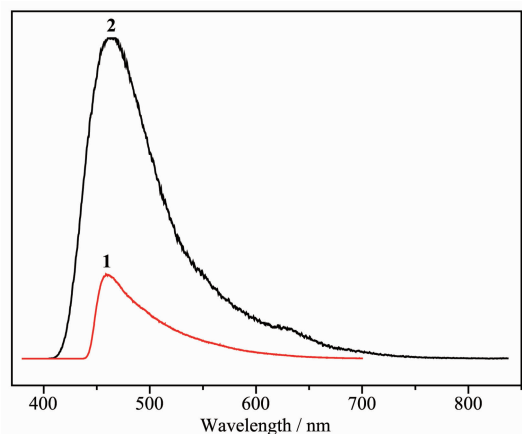


Fig.7 Solid-state emission spectra of the complexes **1** and **2**

3 Conclusions

In conclusion, two coordination polymers based on H₂bpdc and 1,3-bip mixed ligands have been prepared under solvothermal conditions. By changing the central ion, two new complexes with different structures were constructed. Complex **1** features a 3D → 3D fivefold interpenetrating framework via the connectivity among cationic [Zn(1,3-bip)]₂⁴⁺ macrocycles

and bpdc²⁻ ligands. Complex **2** features a 2D → 2D (4,4) net. In addition, the photoluminescence investigation shows that two coordination polymers appear potentially applied as luminescent materials. Further experiments exploring the structural effects of the spacer length of bis(imidazole) ligands on coordination polymers, and any resulting changes in physico-chemical properties, are underway in our laboratory.

References:

- [1] Eddaoudi M, Moler D B, Li H L, et al. *Acc. Chem. Res.*, **2001**,**34**:319-330
- [2] Halder G J, Kepert C J, Moubaraki B, et al. *Science*, **2002**, **98**:1762-1765
- [3] Dybtsev D N, Chun H, Yoon S H, et al. *J. Am. Chem. Soc.*, **2004**,**126**:32-33
- [4] Kesanli B, Cui Y, M. Smith R, et al. *Angew. Chem. Int. Ed.*, **2005**,**44**:72-75
- [5] Ghosh A K, Jana A D, Ghoshal D, et al. *Cryst. Growth Des.*, **2006**,**6**:701-707
- [6] Gong Y, Li J, Qin J B, et al. *Cryst. Growth Des.*, **2011**,**11**: 1662-1674
- [7] Guo Q Q, Xu C Y, Zhao B, et al. *Cryst. Growth Des.*, **2012**, **12**:5439-5446
- [8] Mu Y Y, Han G, Li Z, et al. *Cryst. Growth Des.*, **2012**,**12**: 1193-1200
- [9] Zuo Y, Fang M, Xiong G, et al. *Cryst. Growth Des.*, **2012**,**12**: 3917-3926
- [10] Reger D L, Leitner A, Smith M D. *Inorg. Chem.*, **2013**,**52**: 10041-10051
- [11] Xi X B, Liu Y, Cui Y. *Inorg. Chem.*, **2014**,**53**:2352-2354
- [12] Xie Y B, Gan L, Saudo E C, et al. *CrystEngComm*, **2015**,**17**: 4136-4142
- [13] Anokhina E V, Vougo-Zanda M, Wang X Q, et al. *J. Am. Chem. Soc.*, **2005**,**127**:15000-15001
- [14] Wang R H, Han L, Jiang P L, et al. *Cryst. Growth Des.*, **2005**,**5**:129-135
- [15] Xu X X, Lu Y, Wang E B, et al. *Cryst. Growth Des.*, **2006**, **6**:2029-2035
- [16] Wang Y B, Zheng X J, Zhuang W J, et al. *Eur. J. Inorg. Chem.*, **2003**,**12**:3572-3578
- [17] Yang Y, Du P, Ma J F, et al. *Cryst. Growth Des.*, **2011**,**11**: 5540-5547
- [18] Zhu S R., Zhang H, Zhao Y M, et al. *J. Mol. Struct.*, **2008**, **892**:420-426
- [19] Qua H, Qiu L, Leng X K, et al. *Inorg. Chem. Commun.*,

- 2011,14**:1347-1352
- [20]Wu Y P, Li D S, Zhao J, et al. *CrystEngComm*, **2012,14**: 4745-4750
- [21]Han M L, Wang J G, Ma L F, et al. *CrystEngComm*, **2012,14**: 2691-2698
- [22]Sheldrick G M. *SHELXS-97, A Program for the Siemens Area Detector Absorption Correction*, University of Göttingen, Germany, **1997**.
- [23]Sheldrick G M. *SHELXL-97, Program for the Refinement of Crystal Structures*, University of Göttingen, Germany, **1997**.
- [24]Zhao X, He H, Hu T, et al. *Inorg. Chem.*, **2009,48**:8057-8061
- [25]He H, Dai F, Sun D. *Dalton Trans.*, **2009,763**:365-371
- [26]Zhao X, He H, Dai F, et al. *Inorg. Chem.*, **2010,49**:8650-8656
- [27]Nakamoto K. *Infrared and Raman Spectra of Inorganic and Coordination Compound. 5th Ed.* New York: Wiley, **1997**.
- [28]Li X Y, Liu X X, Yue K F, et al. *RSC Adv.*, **2015,5**:81689-81695
- [29]Wen L L, Li Y Z, Lu Z D, et al. *Cryst. Growth Des.*, **2006,6**: 530-537
- [30]Zhang L P, Ma J F, Yang J, et al. *Inorg. Chem.*, **2010,49**: 1535-1550
- [31]Su Z, Fan J, Okamura T, et al. *Cryst. Growth Des.*, **2010,10**: 1911-1922